Vol 18 No 4, April 2009
1674-1056/2009/18(04)/1479-07
Chinese Physics B
© 2009 Chin. Phys. Soc.
and IOP Publishing Ltd

Time-dependent theoretical approach to the influence of laser fields on the resonance enhanced multi-photon ionization of SH radical*

Yue Da-Guang(岳大光), Zheng Xiao-Yun(郑晓云), Liu Hao(刘 浩), Wang Chun-Xing(王春兴), and Meng Qing-Tian(孟庆田)†

College of Physics and Electronics, Shandong Normal University, Jinan 250014, China

(Received 19 May 2008; revised manuscript received 6 August 2008)

This paper reports that the (2+1) resonance enhanced multi-photon ionization spectra of SH radical in external fields are simulated using the split-operator scheme of time-dependent wave-packet method. Two ionic states, i.e. $a^1\Delta$ and $b^1\Sigma^+$, are involved in the simulation. It gives the simulated photoelectron spectra, the population in each electronic state, as well as the projection of the wave-packet in each electronic state on different vibrational states. These results show that the so-called four-state model can represent the experimental results well.

Keywords: photoelectron spectra, time-dependent wave-packet method, four-state model, multi-photon ionization

PACC: 3365, 3280F, 3280k, 3300

1. Introduction

It is known that the mercapto radical (SH) plays an important role in the ultraviolet photochemistry of sulphur-containing species released into the atmosphere from natural and anthropogenic sources. In the astrochemical context, the relative high cosmic abundance of sulfur, and the recently reported first experimental observation of SH in outer space should also spur a renewed interest in this species. Despite its simplicity and importance, some aspects of the electronic structure and dynamics of this molecule are, however, still challenging nowadays. Nevertheless, detailed information of its spectroscopic and photochemical properties is relatively scarce. In 1995, Milan and his co-workers had observed the $[a^1\Delta]5p\pi^2\phi$ state of the SH (SD) radical using resonance enhanced multi-photon ionization (REMPI) photoelectron spectroscopy (PES) method.[1] Subsequently, this group had studied two-photon REMPI PES of the SH (SD) radical below and above the lowest ionization threshold.[2] They had done many experiments and theoretical studies about SH radical. In 2006, Chen *et al* had studied photodissociation of SH radical at 121.6 nm.[3] Although many self-consistent explanations are given, the theoretical simulations of these experimental results are seldom reported.

As a powerful tool to investigate atomic and molecular scattering, time-dependent wave-packet method has also been successfully transplanted to deal with light-matter interaction these years. Its success in simulating the multi-photon ionization of some diatomic molecules, such as NO, RbI, NaI, etc.,[4−7] makes one believe that it can be also used to simulate the (2+1) REMPI process of SH radical in external fields, especially for two ionic states. In the present work, by using this time-dependent wave-packet method,[8] four-state model is applied to represent the PES of SH in strong fields: after an initial wave-packet is prepared in the electronic ground state, it is launched to the excited state by a pump pulse; the PES about two ionic states $a^1\Delta$ and $b^1\Sigma^+$ are obtained by the delayed probe pulse which is subjected to the excited states of the SH radical. The so-called four-state model is also valid for the simulation of SD radical REMPI.

This paper is arranged as follows. In the next section, the time-dependent wave packet dynamical the-

*Project supported by the National Natural Science Foundation of China (Grant No 10574083) and the Natural Science Foundation of Shandong Province of China (Grant No Y2006A23). Partial financial support from the National Basic Research Program of China (Grant No 2006CB806000).

†Corresponding author. E-mail: qtmeng@sdnu.edu.cn

ory is reviewed, and the formulations of some dynamical information are also given. In the third section, the simulated results are presented and discussed. And the last section is the summary.

2. Theory

2.1. Hamiltonian

We consider a process of multi-photon ionization which is induced by a pump pulse and a probe one. The shape of the laser pulses is chosen as

$$E(t) = \{E_1 f(t)\cos(\omega_1 t) + E_2 f(t-\Delta t) \times \cos[\omega_2(t-\Delta t)]\}\hat{e}, \quad (1)$$

where E_1 and E_2 are the electric field amplitudes of the pump and probe pulses with the linearly polarized direction $\hat{e}$, respectively, ω_1 and ω_2 the corresponding angular frequencies, Δt the delay time between the two Gaussian pulses. The envelopes $f(t)$ and $f(t-\Delta t)$ of the pulses are expressed as

$$f(t) = \exp\left(-\left(\frac{t}{\tau_1}\right)^2\right),$$
$$f(t-\Delta t) = \exp\left(-\left(\frac{t-\Delta t}{\tau_2}\right)^2\right), \quad (2)$$

where τ_1 and τ_2 denote, the full-widths at half-maximum (FWHM) of pump and probe pulses, respectively. In the experiment of Milan *et al*,[1] an intense pump pulse induces a transition and prepares a coherent superposition of eigenstates, i.e. a wave-packet, via the two-photon excitation. The dynamics of the wave packet is then probed with a second, time-delay weak pulse. The kinetic-energy spectrum of the ejected electron is subsequently analysed as a function of the delay time. At the same time the potential energy curves for all the dipole accessible electronic states and the ground electronic state of the ion have been well characterized. Using the Born–Oppenheimer approximation and neglecting the coupling between the core and photoelectron, we can write the field-free Hamiltonian as

$$\hat{H} = -\frac{\hbar^2}{2\mu}\frac{\partial^2}{\partial R^2} I + \hat{U}(R,t), \quad (3)$$

where R is the internuclear separation, I the identity matrix, μ the reduced mass of the molecule, and $\hat{U}(R,t)$ the potential matrix. For a four-state model X, A, C and D, the potential matrix can be written as

$$\hat{U}(R,t) = \begin{pmatrix} V_{\rm X} & W_{\rm AX} & 0 & \dots & \dots & \dots & \dots & 0 \\ W_{\rm AX} & V_{\rm A} & W_{\rm AC} & \dots & W_{\rm AC} & W_{\rm AD} & \dots & W_{\rm AD} \\ 0 & W_{\rm AC} & V_{\rm C}+E_{\rm I,1} & 0 & 0 & 0 & \dots & 0 \\ \vdots & \vdots & 0 & \vdots & \vdots & \vdots & \vdots & \vdots \\ 0 & W_{\rm AC} & 0 & 0 & V_{\rm C}+E_{{\rm I},n} & 0 & \vdots & \vdots \\ 0 & W_{\rm AD} & 0 & 0 & \vdots & V_{\rm D}+E_{\rm I,1} & 0 & 0 \\ \vdots & \vdots & \vdots & \vdots & \vdots & 0 & \dots & 0 \\ 0 & W_{\rm AD} & 0 & 0 & 0 & 0 & 0 & V_{\rm D}+E_{{\rm I},n} \end{pmatrix}, \quad (4)$$

where V_i (i=X, A) refer to the potential energies of two neutral electronic states, $V_{\rm C} + E_{{\rm I},j}$ and $V_{\rm D} + E_{{\rm I},j}$ ($j = 1, 2, \dots, n$) denote the potential energies of the two sets of 'discrete' continuum states in the part of ion-pair states, with $E_{{\rm I},j}$ ($j = 1, 2, \dots, n$) the electron kinetic energies, n the number of the bases in the part of C and D states.

2.2. Solution of the time-dependent Schrödinger equation

Within the Born–Oppenheimer approximation, the time-dependent Schrödinger equation can be written as

$$\mathrm{i}\hbar\frac{\partial}{\partial t}\Phi(R,t) = \hat{H}(R,t)\,\Phi(R,t). \quad (5)$$

Once the Hamiltonian is given, the time-dependent Schrödinger equation can be solved through the split-operator technique of wave-packet method. For simplicity, we here only give the synopsis of the method below. For more details, the reader is referred to the review articles[9−12] and the references therein.

Denote the small time interval Δt, the canonical solution of Eq.(5) is written as

$$\Phi(R, t+\Delta t) = \exp\left(-\frac{\mathrm{i}}{\hbar}\hat{H}\Delta t \right) \Phi(R, t). \quad (6)$$

According to the split-operator scheme, the wave packet can be propagated and evolved as

$$\Phi(\boldsymbol{R}, t_0+\Delta t) \approx U_T^{1/2}(\boldsymbol{R}, t_0) U_V(\boldsymbol{R}, t_0) U_T^{1/2}(\boldsymbol{R}, t_0) \times \Phi(\boldsymbol{R}, t_0), \quad (7)$$

where U_V and U_T are two evolution operators, which represent the evolutions of kinetic energy and potential energy, respectively. After propagating many steps, the wave function of the electronic states and electron-ion pair states in any time will be got. So the wave function has the following approximative form:

$$\Phi(R, t_0+m\Delta t) = \left[\prod_{k=0}^{m-1} U_T U_V(R, t+k\Delta t) \right] \Phi(R, t_0). \quad (8)$$

Since as we know, U_T and U_V can be diagonalized in momentum and coordinate spaces, respectively, it is natural that when meeting operator U_T in calculation, the wave function should be transformed into one in momentum space; when meeting operator U_V, on the other hand, the wave function should be transformed back into one in coordinate space. The process is performed by the so-called Fourier transform (FT), i.e.

$$F[f] = \frac{1}{\sqrt{2\pi}} \int_{-\infty}^{+\infty} \mathrm{d}R' \exp(\mathrm{i}kR') f(R'). \quad (9)$$

In such a way

$$U_T^{1/2} \Phi(R, t) = F^{-1} \exp\left[-\mathrm{i}\Delta t \frac{\hbar k^2}{4\mu} \right] F \Phi(R, t_0). \quad (10)$$

In the split-operator scheme, the general FT is replaced by the FFT (fast Fourier transforms). Because the initial state is a bound state in the problem considered, it can be taken as the eigenfunction of ground vibration state for the ground electronic state. By analysing the nuclear wave packet $\Phi_i\ (R, t)$ $(i = \mathrm{X},\ \mathrm{A}, \ldots)$, such dynamical information as the population in each state and the PES, etc., can be extracted. Take the molecule's PES of the multi-photon ionization in the strong field as an example. It can be expressed as follows:

$$P(E_j, t) = \int \mathrm{d}R \Phi^*_{\mathrm{I,E_j}}(R, t) \Phi_{\mathrm{I,E_j}}(R, t) \quad (11)$$

with $j = 1, 2, \ldots$ being the related electron-ionic states, and the total ion signal P_{Ion} is then given by the sum of $P(E_j, t)$ over all possible kinetic energies for the ejected electron

$$P_{\mathrm{Ion}}(t) = \sum_j P(E_j, t). \quad (12)$$

For different electronic state, the projection of the calculated wave-packet on each vibrational state ϕ_{k_i} can be written as

$$P_{\mathrm{pri}} = \int \mathrm{d}R \phi^*_{k_i}(R) \Phi_k(R, t) \quad (13)$$

with electronic state symbol $k = \mathrm{X}, \mathrm{A}, \ldots$ and the relevant vibrational quantum number $i = 0, 1, 2, \ldots$. Other dynamical information can be also obtained in the same way.[13]

3. Results and discussions

In Milan's experiment, four typical electronic states are involved in the multi-photon ionization of SH radical. We denote them as $X^2\Pi$, $[b^1\Sigma^+]4p\sigma^2\Sigma^+$, $a^1\Delta$ and $b^1\Sigma^+$ states. The ground state $X^2\Pi$ has a $(1\sigma)^2(2\sigma)^2(3\sigma)^2(1\pi)^4(4\sigma)^2(5\sigma)^2(2\pi)^3$ electronic configuration. Removal of an electron from the 2π molecular orbital, which consists essentially of the non-bonding $3p_x$ and $3p_y$ orbitals centred on the sulfur atom, gives rise to three different ionic states, the $X^3\Sigma^-$ ground ionic state, the $a^1\Delta$ and $b^1\Sigma^+$ excited ionic states, which are located at 10.42 eV, 11.65 eV, and 12.76 eV above the ground state of the neutral radical,[1] respectively. A summary of their spectroscopic parameters is given in Table 1. To represent the PES of the SH radical, we performed the four-state (ground state, excited state, and two ionic states, and since ionic ground state $X^3\Sigma^-$ is far from the resonance region, it is not considered here) quantum mechanical calculations. In what follows, we will assign these states as X, A, C, D and refer to them as the four-state model (Fig.1). The related potential parameters can be seen in Table 1.

Table 1. Potential parameters of SH radical in Fig.1, 1 Å=0.1 nm.

Electronic state	IP/cm^{-1}	B_0	ω_e/a.u.	$\omega_e\chi_e$	D_e/cm^{-1}	r/Å
$X^2\Pi$		9.5482[c]	2704.2[c]	51.88[c]	30136[b]	1.34385
$[b^1\Sigma^+]4p\sigma^2\Sigma^+$		8.609[a]			2258.3316	1.414753
$X^3\Sigma^-$	84057.5[a]	9.134[a]	2547.7[a]	49.3[a]	32914.682	1.3735
$a^1\Delta$	93925[a]	9.187[a]	2556[b]	45[d]	36295.2	1.3695
$b^1\Sigma^+$	102916[a]	9.164[a]	2563[b]	47[d]	34941.3245	1.371243

[a]Refs.[1, 2], [b]Refs.[14–16], [c]Refs.[17, 18], [d]Refs.[19].

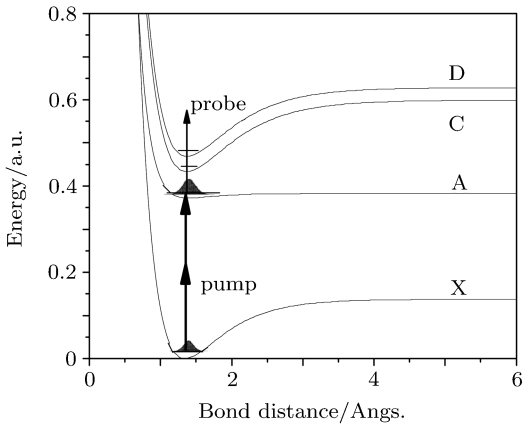


Fig.1. Four-state model: X, A denote states $X^2\Pi$, $[b^1\Sigma^+]4p\sigma^2\Sigma^+$; C, D denote ionic states $a^1\Delta$ and $b^1\Sigma^+$. An intense pulse induces a wave packet in an excited electronic state. The wave packet's motion is probed by a second time-delay laser pulse which is used to ionize the molecule.

The potential energy curves for SH radical and SH^+ electronic states are taken from Refs.[1–3, 14–19]. In the calculation, the relevant dipole moment transition matrix elements are obtained by fitting to *ab initio* results. Since the absolute value of the transition dipole moment for the ion transition is unknown, motivated by the fact that the coupling between bound states and the continuum is much smaller than that between bound states, we always set it to be a factor 10 which is lower than that between the ground and excited states.[4] For convenience to compare with the experiment, the pump-probe delays are set to be from 10 ns to 30 ns, and the number of ion-pair states $n = 60$ is found to be suitable for convergence of calculation. Figure 2 is the PES of SH radical simulated by using the above theory and the four-state model. From it one can see that there exist two peaks in the PES, whose positions are at 2.54 eV and 3.38 eV, respectively, and there is a highest major peak appeared when delay time is 20 ns, the intensity of the pump pulse is 5.0×10^{13} W/cm^2, and the probe pulse is 2.0×10^{12} W/cm^2. The simulation shows that these two peaks correspond to the ionization from excited states D and C.

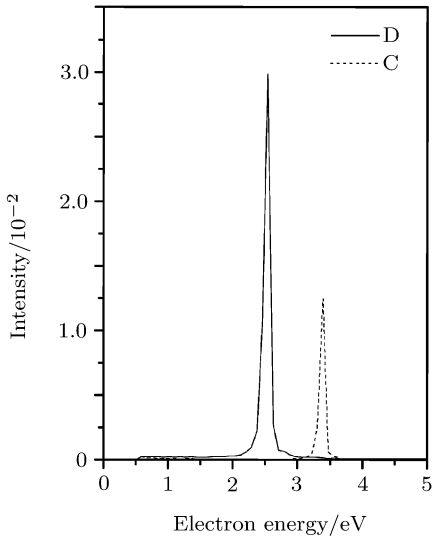


Fig.2. The PES of SH radical. The two calculated peaks are located at 2.54 eV and 3.38 eV, respectively, which correspond to the ionization from excited states D and C.

To show which vibrational states in $a^1\Delta$ and $b^1\Sigma^+$ are populated by the probe pulse from the excited state $[b^1\Sigma^+]4p\sigma^2\Sigma^+$, we calculated the projection of the wave packet in $a^1\Delta$ and $b^1\Sigma^+$ states on their each vibrational state (Fig.3). It is found that there is more population in D state than that in C state, which can be attributed to the stronger coupling between the neutral excited state A and ionic state D. In addition, it is easily understood that because of being far from the resonance region, except for the first three vibrational states, others have very little population. This results are shown to be in good agreement with the experimental ones.[2] Certainly, we can guess that the vibrational population in the electronic ground state is also disturbed by the pump pulse, which has been proved by the simulated results displayed in Fig.4. Obviously, if we choose the initial wave-packet as the ground vibrational state of the

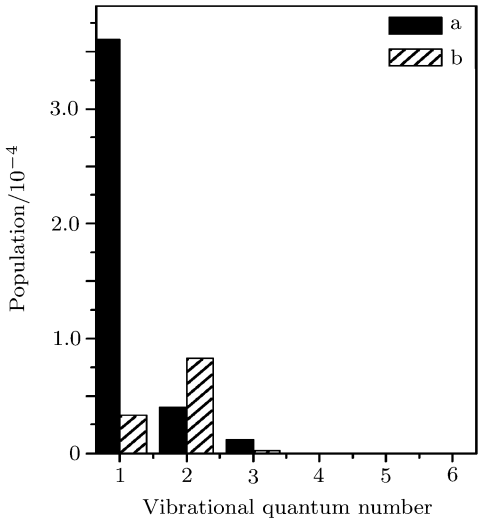


Fig.3. The projection of wave-packet in ionic states D (a) and C (b) on relevant different vibrational states.

electronic state (Fig.4(a)), its projection on each vibrational state will be changed greatly after the pump pulse is over (Fig.4(b)). Owing to part of the particles has been excited to the upper state, the magnitude of the total population is less than one before the pump pulse is subjected. The same tendency can be found in Fig.5, which gives the population on each electronic state changing with evolution time and laser intensity.

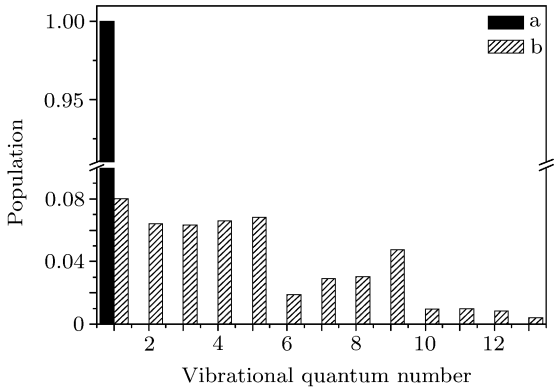


Fig.4. The population of ground state of SH radical when the pulse is absent. (b) The population of ground state of SH radical when the pulse is over.

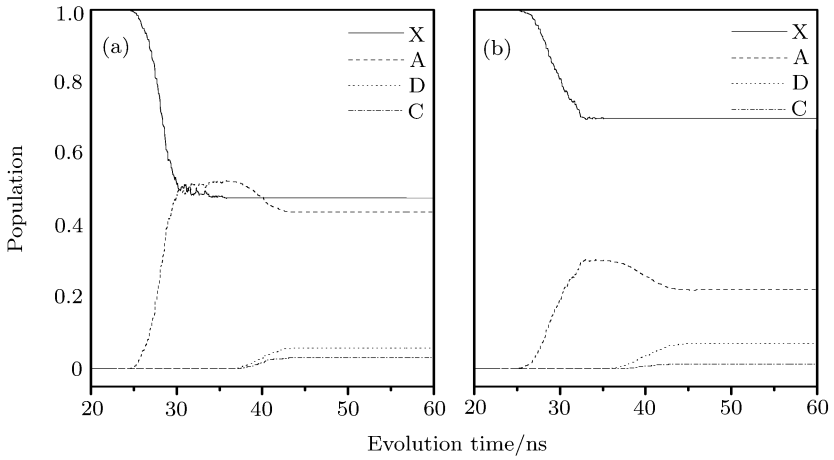


Fig.5. The comparison of the population in each electronic state for different intensities. The intensity of pump and probe pulse is, respectively, 5.0×10^{13} W/cm^2 and 2×10^{12} W/cm^2 for (a); 5.0×10^{12} W/cm^2 and 2×10^{12} W/cm^2 for (b).

To illustrate the influence of pulse intensity on PES, we performed a simulation for different laser intensities, which is displayed in Fig.6. Obviously, the peak heights of the PES increases with the increase of both pump and probe pulse intensities. Since the laser intensity affects the population of each electronic state (Fig.5), the phenomena are easy to be understood. As for the influence of delay time on the PES, it can also be translated into the influence of laser intensity. In the region of pulse overlap, with the delay time becoming smaller, the overlap extent of two pulses increases. According to what is mentioned above, the intensity of PES will become larger. But the increase of pulse intensity does not imply the intensity of PES being always increasing (Fig.7), which is consistent with the conclusion of Ref.[20]. What is more interesting in Fig.7 is that with the decrease of the delay time, apart from the two peaks located at 2.54 eV and 3.38 eV, there will be two more peaks appeared in the PES. This phe-

nomenon can be easily explained by the new formed sum frequency component and difference frequency one induced by the overlap or partial overlap of pump and probe pulses: because of the vibrational redistribution of the neutral and ionic ground electronic state, the sum frequency component will induce a peak at about 5.07 eV, while the difference frequency component will induce a peak at about 0.70 eV. Since these two components have the largest strength when delay time is zero, they give the largest contribution to the PES in this situation. When the delay time is larger, with disappearance of the pulses overlap, these two peaks also disappear. We notice also that when the delay time is 20 ns, the two major peaks at about 2.54 eV and 3.38 eV have the highest height (Fig.8). This phenomenon can be illustrated by that at this delay time, the evolution of the wave-packet on the neutral excited state will make it to have a most favoured population being ionized.

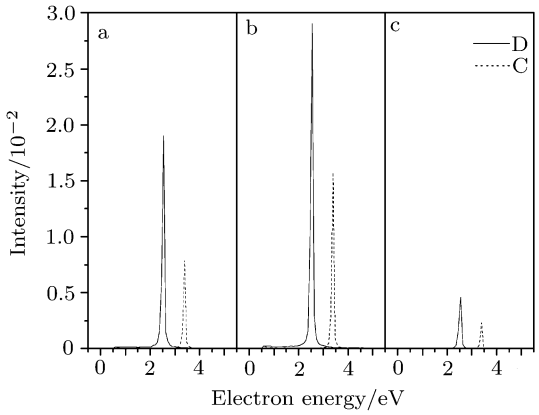


Fig.6. The changing behaviour of PES with intensity of the pump and probe pulses. The intensity of pump and probe pulse is, respectively: 5.0×10^{12} W/cm^2 and 2×10^{12} W/cm^2 for (a); 5.0×10^{13} W/cm^2 and 2×10^{12} W/cm^2 for (b); 5.0×10^{13} W/cm^2 and 2×10^{11} W/cm^2 for (c).

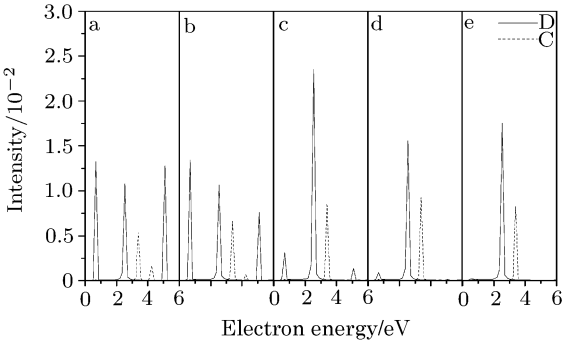


Fig.7. The changing behaviour of PES with delay time. The intensity of the pump and probe pulse is 5.0×10^{12} W/cm^2 and 2×10^{12} W/cm^2, respectively. a, b, c, d, e correspond to delay time 0 ns, 2 ns, 4 ns, 6 ns, and 8 ns respectively.

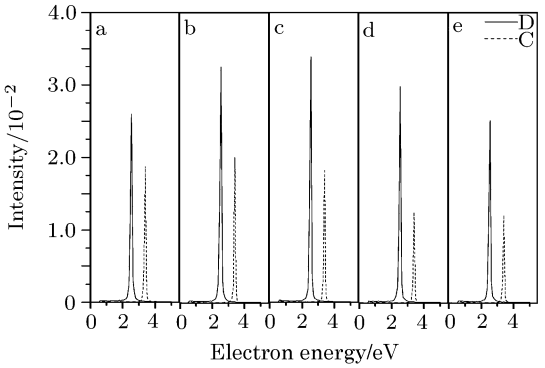


Fig.8. The changing behaviour of PES with delay time. The intensity of the pump and probe pulse is 5.0×10^{12} W/cm^2 and 2×10^{12} W/cm^2, respectively. a, b, c, d, e correspond to delay time 10 ns, 15 ns, 20 ns, 25 ns, and 30 ns, respectively. The peak of the population is the highest when the delay time is 20 ns.

4. Summary

In this paper, using the time-dependent wave-packet method, we simulated the photoelectron spectra of the SH radical for the (2+1) ionization process via the neutral excited state $[b^1\Sigma^+]4p\sigma^2\Sigma^+$ in strong fields. It is found that since the laser intensity affects the population in each electronic state, it naturally affects the shape and the peak position of the photoelectron spectra. As for the influence of pulse delay time, it can also be ascribed to the effect of laser intensity. Special attention should be paid to the existence of appearing minor peaks when delay time is smaller than the pulse width. We attribute it to the influence of new formed 'pulse' owing to the pulse overlap. This kind of intense field effect may be instructive for controlling chemical reaction.

References

[1] Milan J B, Buma W J, deLange C A, Western C M and Ashfold M N R 1995 *Chem. Phys. Lett.* **239** 326

[2] Milan J B, Buma W J and deLange C A 1996 *J. Chem. Phys.* **105** 6688

[3] Chen S P, Zhou W D and Zhang J S 2006 *Chem. Phys. Lett.* **418** 328

[4] Meng Q T, Yang G H, Sun H L, Han K L and Lou N Q 2003 *Phys. Rev.* A **67** 063202

[5] Liu C H, Meng Q T and Zhang Q G 2006 *Chem. Phys. Lett.* **326** 344

[6] Miao X Y, Wang L and Song H S 2007 *Phys. Rev.* A **75** 042512
[7] Yao G X, Wang X L, Du C M, Li H M, Zheng X F, Ji X H and Cui Z F 2006 *Acta Phys. Sin.* **55** 2210 (in Chinese)
[8] Bai L H, Liu X G and Zhang Q G 2003 *Acta Phys. Sin.* **52** 2774 (in Chinese)
[9] Bandrauk A D and Hai S 1991 *Chem. Phys.* **176** 428
[10] Feit M D and Fleck J A 1983 *J. Chem. Phys.* 78 301
[11] Cooley J W, and Tuckey J W 1965 *Math. Comput.* **19** 297
[12] Feit M D, Fleck Jr J A and Steiger A 1982 *J. Comput. Phys.* **47** 412
[13] Zhang H, Han K L, He G Z and Lou N Q 1998 *Chem. Phys. Lett.* **289** 494
[14] Ramsay D 1952 *J. Chem. Phys.* **20** 1920
[15] Ashold M N R, Tucher B and Western C M 1989 *Mol. Phys.* **66** 981
[16] Rostas J, Horani M, Brion J, Daumont D and Malicet 1984 *J. Mol. Phys.* **52** 1431
[17] Stella M Resende and Fernando R Ornellas 2001 *J. Chem. Phys.* **115** 2178
[18] Ramsay D A 1952 *J. Chem. Phys.* **9** 1920
[19] Levick A P and Sarre P J 1989 *J. Mol. Spectrosc.* **133** 227
[20] Meng Q T, Liu X G, Zhang Q G and Han K L 2005 *Chem. Phys.* **316** 93